Earth Syst. Dynam. Discuss., doi:10.5194/esd-2016-72, 2017
Manuscript under review for journal Earth Syst. Dynam.
Published: 2 January 2017

Earth System Dynamics
Discussions
Open Access

Return Levels of Temperature Extremes in Southern Pakistan

Maida Zahid[1], Richard Blender[1] ,Valerio Lucarini[1,2] and Maria Caterina Bramati[3]

1. Meteorological Institute, University of Hamburg, Hamburg Germany
2. Department of Mathematics and Statistics, University of Reading, Reading, UK
3. Department of Statistical Science, Cornell University, New York, United States

Correspondence to: Maida Zahid (maida.zahid@uni-hamburg.de)

Abstract. Southern Pakistan (Sindh) is one of the hottest regions in the world and is highly vulnerable to temperature extremes. In order to improve rural and urban planning, information about the recurrence of temperature extremes is required. In this work, return levels of the daily maximum temperature T_{max} are estimated, as well as the daily maximum wet-bulb temperature TW_{max} extremes. The method used is the Peak Over Threshold (POT) and it represents a novelty among the approaches previously used for similar studies in this region. Two main datasets are analyzed: temperatures observed in nine meteorological stations in southern Pakistan from 1980 to 2013, and the ERA Interim data for the nearest corresponding locations. The analysis provides the 2, 5, 10, 25, 50 and 100-year Return Levels (RLs) of temperature extremes. The 90% quantile is found to be a suitable threshold for all stations. We find that the RLs of the observed T_{max} are above 50°C in northern stations, and above 45°C in the southern stations. The RLs of the observed TW_{max} exceed 35°C in the region, which is considered as a limit of survivability. The RLs estimated from the ERA Interim data are lower by 3°C to 5°C than the RLs assessed for the nine meteorological stations. A simple bias correction applied to ERA Interim data improves the RLs remarkably, yet discrepancies are still present. The results have potential implications for the risk assessment of extreme temperatures in Sindh.

Key words
Extreme temperature, return levels, peak over threshold, Generalized Pareto Distribution, declustering.

1 Introduction

Extreme maximum temperature events have received much attention in recent years, because of the associated risk of mortality and their likely increase in intensity and frequency in climate change scenarios (Sheridan and Allen, 2015). An example of the potential impact of raising maximum temperatures is the recent heat wave in Southern Pakistan (Sindh), which occurred between June 17th and June 24th 2015 and broke all the records with a death toll of 1400 people, and over 14000 people hospitalized. The temperatures in different cities of the Sindh region were in the range of 45°C - 49°C during the event (Imtiaz and Rehman, 2015). Karachi had the highest number of fatalities (1200 people approximately). The Pakistan Meteorological department issued a technical report stating a very high heat index (measuring the heat stress on humans due to high temperature and relative humidity) during this heat wave (Chaudhry et al., 2015).

In summer, Sindh becomes very hot and with the arrival of a monsoon the humidity increase in the region (Chaudhry and Rasul, 2004). This lethal combination of high temperature and relative humidity is known as wet-bulb temperature, which increases the death rates, and severely impacts the human habitability (Pal and Eltahir 2015). The human body generally maintains the temperature around 37°C. However, the human skin regulates at or below 35°C to release heat (Sherwood and Huber, 2010). Under high levels of the moisture content in the atmosphere, the human body cannot maintain the skin temperature below 35°C and can develop ailments like hyperthermia, heat strokes and cardiovascular problems. Hyperthermia can occur even in the fittest human beings, if they are exposed to an environment where wet-bulb temperature is greater than 35°C for at least six hours. Hyperthermia is a condition where extremely high body temperature is reached, resulting from the inability of the body to get rid of the excess heat. It occurs mostly when temperature and relative humidity levels are extremely high at the same time.

This study devotes special attention to Sindh because of its exposure to the frequent and intense temperature extremes in the past (Zahid and Rasul, 2012). This region is considered as one of the most vulnerable regions in Pakistan. Sindh stretches from 23.5° N – 28.5° N and 66.5°E - 71.1°E, and is bounded on the west by the Kirthar Mountains, to the north by the Punjab plains, to the east by the Thar desert and to the south by the Arabian Sea (Indian Ocean) and in the center fertile land around Indus river. The Indus river is the source of water for the agriculture lands. Cotton, wheat and sugar cane are grown on the left bank of the Indus and rice, wheat and gram on the right bank (Chaudhry and Rasul, 2004). Cotton is the cash crop of the country.

The climate in Sindh is arid and subtropical with less than 250 mm annual rainfall. The temperature frequently exceeds 45°C in summer (May-September) and the minimum average temperature recorded during winter (December- January) is 2°C. Table 2 shows the mean monthly climatic characteristics of the region from 1980-2010. Figure 1 shows the spatial distribution of all nine weather stations of Pakistan meteorological department, and the ERA Interim grid points close to the corresponding locations. High population density, limited resources, poor infrastructure and high dependence of the local agriculture on climatic factors, mark this region as highly vulnerable to the impacts of climate change.

The Intergovernmental Panel on Climate Change (IPCC) scenarios estimates for this region an increase in the surface temperature of the order of 4°C in this region by the end of 2100. This may significantly reduce crop yields, and cause huge economic losses to the country (Islam et al., 2009; Rasul et al., 2012; IPCC, 2012; Pachauri et al., 2014). Furthermore, it might increase the risks of heat strokes, cardiac arrest, high fever, diarrhea, cholera and vector borne diseases. Heat waves became more frequent and intense during 90's in Southern Pakistan. Zahid and Rasul (2010) reports the significant rise in heat index and heat waves events longer than ten days in Sindh. The enhanced mortality rate related to the heat waves is a serious problem, and two obvious examples are the 1991 and the previously mentioned 2015 heat waves (Imtiaz and Rehman, 2015).

The analysis of extreme climatic events is a very active area of research in geosciences (Christidis et al., 2005, 2010; Tebaldi et al., 2006; Zwiers et al., 2011; Morak et al., 2011, 2013). In order to facilitate and standardize the analysis of extremes, the World Meteorological Organization (WMO) has suggested 27 specific climate indices, like the number of hot days, cold days, wet days, dry days, etc. (Tank et al., 2006; 2009, Frisch et al., 2002; Choi et al., 2009; Lustenberger et al., 2014). The investigation and analysis of such climate indices has now reached a high level of popularity.

Extreme value theory (EVT) represents an increasingly widespread approach in climate studies (Coles, 2001, Zhang et al., 2004; Brown et al., 2008; Faranda et al., 2011; Acero et al., 2014) to estimate the occurrence of the extreme events. The peak over threshold (POT) approach determines the distribution of the exceedances above a threshold. The exceedances are asymptotically distributed according to the Generalized Pareto Distribution (GPD). GPD has remarkable properties of universality when the asymptotic behavior is considered (Lucarini et al., 2016), while one can expect that the threshold level above which the asymptotic behavior is achieved depends on the specifics of the analyzed time series. In particular, when looking at spatial fields, it will depend on the geographical location.

In this study, we have chosen to use the POT method to assess the temperature extremes in the Sindh region, because it is the most practical approach in modeling the risks of extremes. It is applied for studying temperature extremes in different regions of the world (Burgueño et al., 2002; Nogaj et al., 2006; Coelho et al., 2008; Ghill et al., 2011). However, to our knowledge, the POT method has never been used to analyze the risk of temperature extremes in Sindh. The POT approach allows in principle for estimating the return periods and the return levels (RLs) also for time ranges longer than what has been currently observed. This information and this predictive power can be beneficial for policy makers and other stakeholders. Note that this is exactly the kind of information planners need when, e.g., designing infrastructures that are deemed to last a very long time.

It is useful to consider two indicators of extreme temperatures: (1) temperature extremes T_{max}, and (2) Wet-bulb temperature extremes TW_{max}, and are interlinked, but rarely studied together. The southern Pakistan (Sindh) lacks the information about both the temperature extremes and faces the consequences of heat waves almost every year. Thus, considering the need and relevance of the information such a study is necessary and timely.

Therefore, we estimate the return levels of extreme daily maximum temperatures T_{max} and daily maximum wet-bulb temperatures TW_{max} over the different return periods in Sindh. We apply the peak over threshold (POT) method on the observational data of the nine weather stations provided by Pakistan meteorological department, and the ERA Interim data of European center for medium range weather forecast (ECMWF) model for the corresponding grid points from 1980 to 2013. If the ERA Interim dataset characterizes well the extremes, it could be an option for the regions inside Sindh where no observational data is available. Furthermore, a standard bias correction is applied on the ERA Interim data to improve the results.

The paper is organized as follows. In Section 2, the statistical modeling of extremes using peak over threshold method is briefly illustrated along with a description of the data used. The estimation of daily maximum wet-bulb temperature is discussed in detail in this Section. Section 3 presents the main results of the POT analysis on the meteorological station observations, ERA Interim, and bias corrected ERA Interim daily maximum temperature T_{max} and wet-bulb temperature TW_{max} data at nine locations, viz. Jacobabad, Mohenjo-daro, Rohri, Padidan, Nawabshah, Hyderabad, Chhor, Karachi, and Badin. The performance of the ERA Interim and bias corrected ERA Interim in comparison to observations is also described in Section 3. All computations and graphics in this work are done using the R free open source statistical software, using the packages ismev and extRemes (see www.R-project.org and R Development core team 2015). Section 4 summarizes the major findings of the study and concludes our work.

2. Data and Methodology

2.1 Meteorological Station Data

The daily maximum temperature and relative humidity data recorded at nine meteorological stations in Sindh from 1980 to 2013 are provided by the Pakistan Meteorological Department (see Table 1). We select nine stations, which contain a negligible amount of missing values after 1980, and are suitable for the POT analysis. An additional criterion is that only those stations are chosen where no changes occurred in measuring instruments during the last 33 years (Brunetti et al., 2006). None of the station data shows gaps with a duration longer than two days, which are treated by replacing the missing values with the average of the two previous values.

The temperature data are discretized unevenly with intervals up to 1 degree Celsius. Deidda and Puliga (2006) uses a Monte Carlo study for simulating various resolutions to show that the discretization in precipitation data affects the convergence of parameter estimation in the extreme value analysis. For this reason, we produce high resolution data to compensate the effect of discretization and thus to improve the convergence of the estimator. To convert station data to higher resolution, we add them to a uniform noise with the magnitude corresponding to the discretization steps (1 degree C). The noise r is a uniform random variable in the interval [-0.5, 0.5]. The main property of this noise is to round (T+r) = T, where T is the temperature with 1-degree resolution and 'round' is the numerical function, which maps the interval [T-0.5, T+0.5] to T. Thus, adding the noise does not perturb the information content of the observations. This procedure is applied to all temperature data, irrespective of the actual resolution, and replicated 100 times using a Monte Carlo approach. Results are then averaged. We check the influence of this noise parameterization and find no significant bias in the return level estimates.

2.2 ERA Interim Reanalysis Data

The gridded daily maximum temperature and relative humidity data of ERA Interim reanalysis is downloaded from the website ECMWF Public Datasets web interface (http://apps.ecmwf.int/datasets/). The ERA Interim is produced from the European center for medium range weather forecast (ECMWF) model with resolution 0.75° × 0.75° (Dee et al., 2011). The gridded data is then extracted at the closest grid point of all stations, for the period 1980-2013. The latitude and longitude of the ERA Interim stations are displayed in Table 1.

One of the main requirements to perform the POT analysis is a stationary time series. Therefore, similar to Bramati et al. (2014), the ADF test of stationarity (Dickey and Fuller, 1979) is performed on all the time series. The test results show no sign of long-term correlations in the data. High short-term correlations (daily time scale) typically lead to clusters of extreme values and require the use of a declustering method (see more detail in Section 2.4).

2.3 Wet-bulb Temperature Calculations

The wet-bulb temperature measures the heat stress better than other existing heat indices, because it establishes the clear thermodynamic limit on heat transfer that cannot be overcome by adaptations like clothing, activity and acclimatization (Pal and Eltahir 2015, Sherwood and Huber, 2010). Here, we use an empirical equation developed by Stull (2011) to measure the wet-bulb temperature [°C].

$$\mathrm{TW}_{max} = \mathrm{T}_{max}\ \mathrm{atan}\,(\alpha_1\sqrt{\mathrm{RH}_{max}+\alpha_2}) + \mathrm{atan}(\mathrm{T}_{max}+\mathrm{RH}_{max}) - \mathrm{atan}(\mathrm{RH}_{max}+\alpha_3) + + \alpha_4(\mathrm{RH}_{max})^{\frac{3}{2}}\,\mathrm{atan}(\alpha_5\mathrm{RH}_{max}) - \alpha_6 \qquad (1)$$

where TW_{max} is the maximum wet-bulb temperature [°C], T_{max} is the maximum temperature [°C], and RH_{max} is the maximum relative humidity [%]. This relationship is based on an empirical fit, as in Stull (2011), where the coefficient values are α_1 = 0.151977, α_2 = 8.313659, α_3 = -1.676331, α_4 = 0.00391838, α_5 = 0.023101, and α_6 = 4.686035. The Eq. (1) covers a wide range of relative humidity and air temperatures with an accuracy of 0.3°C.

2.4 Peak Over Threshold

In order to determine return levels (RLs) of extreme maximum temperatures and maximum wet-bulb temperatures in Sindh, the Peak Over Threshold approach (POT) is applied to the meteorological stations, the ERA Interim, and the bias corrected ERA Interim data. In this analysis, extremes are defined as exceedances over threshold distributed according to the Generalized Pareto Distribution (GPD), which is characterized by two parameters, the shape ξ and the scale σ. The GPD for exceedances $x - u$ of a random variable x reads as

$$G(x) = 1 - \left[1 + \xi\left(\frac{x-u}{\sigma}\right)\right]^{-\frac{1}{\xi}} \qquad (x > u, \xi \neq 0\,), \qquad (2)$$

where u is the threshold. The choice of the threshold u is done in order to ensure that the model in (2) provides a reasonable fit to exceedances of this threshold. The result for the two parameters shape ξ and scale σ depend on the threshold u (Coles, 2001). The shape parameter ξ determines the tail behavior while the scale parameter σ measures the variability. For a negative shape parameter, $\xi < 0$, the distribution is bounded (beta distribution), for vanishing shape parameter, $\xi = 0$, the distribution is exponential, and for a positive shape parameter, $\xi > 0$, the distribution has no upper bound (Pareto distribution).

In particular, for a negative shape parameters $\xi < 0$ the GPD has an upper bound

$$A_{max} = u - {}^{\sigma}/_{\xi} \qquad (3)$$

$$G(x) = 0 \qquad (x > A_{max}, \xi < 0\,)$$

where A_{max} is an absolute maximum (Lucarini et al., 2014). The choice of the optimal threshold for performing statistical inference from a time series is crucial. A too large value for u would reduce the number of exceedances to a few values, inflating the variance of the estimators and by consequence the analysis would unlikely yield any useful results. On the other hand, a too small value for u would violate the asymptotic nature of the model, with a possible biased estimation and wrong model selection (Coles, 2001).

The threshold selection is the first step in the application of POT approach, and the stability of the shape

Earth Syst. Dynam. Discuss., doi:10.5194/esd-2016-72, 2017
Manuscript under review for journal Earth Syst. Dynam.
Published: 2 January 2017

parameters ξ and the scale parameters σ fitting the GPD is assessed with various thresholds. The threshold chosen for each station is the lowest value which stabilizes the estimates shape parameters ξ and the modified scale parameters σ* (see details later in Section 3.1). The shape ξ, the scale σ and the return levels are estimated using the Maximum Likelihood Estimator (MLE) using the R software (R Development core team 2015), which also provides an standard errors of estimates.

Multi-occurrence is an important characteristic of extreme climatic events and is referred to as clustering. These clusters are consecutive occurrences of above threshold events. It is important to treat the clustered extremes to achieve the independence assumption, which is crucial for the POT model, in order to apply MLE. We treated the clusters using the concept of Extremal Index (EI) (see Newell, 1964, Loynes, 1965, O'Brien, 1974, Leadbetter, 1983, Smith, 1989, Davison and Smith, 1990). The Extremal Index θ measures the degree of clustering of extremes. It ranges between 0 and 1, (θ = 0 means strong clustering, θ = 1 absence of clusters). Leadbetter (1983) interprets 1/θ as the mean number of exceedances in a cluster.

The extremal index θ can be estimated in two separate ways. Here, we apply the 'intervals estimator' automatic declustering by Ferro and Segers (2003). A distinctive property of this method is that it avoids the subjective choice of cluster parameters. The main ingredient is an asymptotic result for times between threshold exceedances. The exceedance times are split into two types, a set of vanishing intra-exceedance times within the clusters, and an exponentially distributed set of inter-exceedance times between clusters. The method is iterative starting with largest return times and stops when a limit for the inter-exceedance times is reached. The standard errors of the estimated parameters is obtained by a bootstrap procedure. In this study, the extremal index value is ≤ 0.5 in all the time series referring to the clusters.

The primary focus of the study is to estimate N - years return levels (RLs) x_N, which is exceeded on the time scale of N years (Coles, 2001) and reads

$$x_N = u + \frac{\sigma}{\xi}\left[(N n_y \zeta_u)^{\xi} - 1\right], \quad (4)$$

where N represents the return period, n_y is the number of observations per year , ζ_u is the probability of an individual observation exceeding the threshold u, the shape parameter is ξ and the scale parameter is σ.

2.5. Bias Correction Method

A simple bias correction is applied to each ERA Interim time series through a rescaling that adjust the first two moments (mean and variance) to the sample moments calculated on the corresponding observations. Therefore, the bias correction is applied to the entire time series and it is not tailored to the extreme events only. The bias corrected ERA Interim time series x is expressed as

Earth Syst. Dynam. Discuss., doi:10.5194/esd-2016-72, 2017
Manuscript under review for journal Earth Syst. Dynam.
Published: 2 January 2017

$$x = \bar{z} + \frac{y_{ERA} - \bar{y}}{\sigma_y} . \sigma_z \quad (5)$$

where y_{ERA} is the ERA Interim time series, $\bar{y}$ and σ_y its mean and standard deviation, whereas $\bar{z}$ and σ_z are the mean and standard deviation of the meteorological station temperatures. The bias corrected ERA Interim time series shows better results compared to the original ERA Interim data. The comparison of extremes as detected in the station observations, in the ERA Interim, and in the bias corrected ERA Interim time series is carried out in Section 3.

3. Results and Discussion

3.1 Threshold Selection

The threshold selection is the first step in a POT analysis. It is essential to choose a threshold that is high enough to be in the asymptotic limit of the distribution of exceedances, but low enough to have ample data for the fit. The threshold selection is performed using diagnostic plots of the modified scale parameter σ* (σ* = σu – ξu) and the shape parameter ξ of the observed, ERA Interim, the bias corrected ERA Interim T_{max}, and TW_{max} in all stations. In GPD, the excesses above a high threshold have same shape but shifted scale. In order to deal with this problem the modified scale σ* is used, because its estimate remains constant above a sufficiently high threshold guaranteeing that the asymptotic properties are obeyed (Sacrrott and MacDonald, 2012).We observe both the modified scale parameter and the shape parameter ξ stability plots carefully. The threshold u is selected as the lowest value where the two parameters are invariant in order to reach the asymptotic limit (Coles, 2001 and Furrer et al., 2010). Figure 2 shows the parameter stability plots of the station observed T_{max} for Karachi only, as an example to explain the threshold selection procedure. We observe that the 90% quantile is an appropriate threshold for all the station observed, the ERA Interim, the bias corrected ERA Interim T_{max}, and TW_{max}.

In addition to diagnostic plots of the modified scale parameter σ* and the shape parameter ξ, the mean residual life plot is used to select the appropriate threshold for the POT analysis. The mean residual life plot is initiated by Davison and Smith, (1990), according to them lowest value of the threshold should be selected when the threshold based mean excesses are consistent. Hence, the threshold is selected when the plot is approximately linear, like in case of Karachi the station observed T_{max} plot appears to be linear and stable at u = 36, indicating u = 36 as the most suitable threshold for Karachi (Figure 3).

3.2 GPD Fit

The goodness of fit is evaluated by means of Quantile-Quantile (Q-Q) plots and hypothesis testing. The Q-Q plot analysis is performed for the stations observed, the ERA Interim, the bias corrected ERA Interim daily T_{max} and TW_{max}. The Q-Q plots of the observed T_{max} show that the GPD fits well in most of the stations. However, in a few stations the empirical values show slight deviation from the modeled values like Jacobabad, Mohenjo-daro, Padidan and Chhor. In spite of minor deviations at some stations, still most of the exceedances have a good fit with the model. The Q-Q plots of the observed TW_{max} also show good GPD fits in all stations.

The Q-Q plots of the ERA Interim T_{max} indicates that the GPD fits are not good. The empirical values of the higher quantiles are deviating from the theoretical quantiles in all stations. However, if the higher quantiles are neglected, then the stations like Jacobabad, Mohenjo-daro, Rohri, Padidan, Nawabshah, Chhor, and Badin shows that the exceedances fit very well. Likewise, the Q-Q plots of the ERA Interim TW_{max} do not show good fits with the GPD model. The Q-Q plots of the bias corrected ERA Interim $T_{max,}$ and TW_{max} show better results than the ERA Interim. We notice that the T_{max} of the ERA Interim and bias corrected ERA Interim fit better than the TW_{max} if the higher quantiles are ignored.

In order to assess the goodness-of-fit, we apply the Kolmogorov-Smirnov (K-S) test and Anderson-Darling (A-D) test to the data of meteorological stations, ERA Interim, bias corrected ERA Interim T_{max} and TW_{max}. The p-values indicate a good performance of the fit procedure. Table 3 displays the results of the K-S and A-D statistics of the T_{max} and TW_{max} in all the data sets.

3.3 Parameter Estimates

Here, we analyze the shape parameter ξ , the scale parameter σ, and threshold u for all considered datasets. The standard errors of the shape ξ and the scale σ parameters are estimated using the Maximum Likelihood Estimation (MLE), and given in Table 4. The spatial distribution of the shape parameter ξ and the scale parameter σ of the GPD in Sindh are shown in Figure 4. The shape parameters ξ are all negative in all datasets at all stations. This is hardly surprising, as meteorological and physical processes make sure that the temperature cannot grow locally without control. Figure 4 displays the bias corrected ERA Interim results only. The observed T_{max} shape parameters ξ are between -0.418 to -0.223, and for TW_{max} within -0.323 to -0.177. The bias corrected ERA Interim T_{max} shape parameters ξ range from -0.305 to -0.002, and TW_{max} are between -0.18 to -0.01.

The scale parameters σ of the observed T_{max} are from 2.08 to 2.76, and the TW_{max} are in a range 1.86 to 2.76. In the ERA Interim analysis, the scale parameter σ of T_{max} is within 1.00 - 1.95, and for TW_{max} within 0.74 -1.75. We observe a difference in the scale parameters of both the observed, the ERA Interim T_{max} and TW_{max}. We find that the scale parameters of the bias corrected ERA Interim data are much closer to those estimated for T_{max} and TW_{max} using the station data. In the bias corrected ERA Interim T_{max} the scale parameters σ are between 1.50 - 2.75, while for TW_{max} are within a range 1.40 – 2.40 (Figure 4).

3.4 Absolute Maxima

Once the shape ξ , the scale σ, and the thresholds u are fixed, it is possible to compute the theoretical absolute maxima using Eq. (3) (Section 2.4). Theoretical absolute maxima can be compared with the observed ones for each station to better understand the signals of warming in Sindh. The daily maximum temperature T_{max} and the maximum wet-bulb temperature TW_{max} (station data, the ERA Interim, and the bias corrected ERA Interim) have negative shape parameter ξ in all stations. This means that according to Eq. (2) in section 2.4, the probability distribution function (pdf) is bounded by the maximum values. These maximum values are the theoretical upper limits predicted by the GPD fit. The analysis shows that the observed absolute maxima T_{max} and TW_{max} in all stations of the three data sets are below the theoretical absolute maximum, as expected (Figure 5). This gives us confidence on the quality of our fit. The following piece of information can also be derived. Assume that one

Earth Syst. Dynam. Discuss., doi:10.5194/esd-2016-72, 2017
Manuscript under review for journal Earth Syst. Dynam.
Published: 2 January 2017

observes in the future an extreme event larger than the maximum inferred in the present dataset; this may suggest some non-stationarity in the most recent portion of the dataset.

3.5 Return Levels

The return levels (RLs) are computed considering various return periods (2, 5, 10, 20, 50, 100-year). The return level plots of the stations observed, the ERA Interim, the bias corrected ERA Interim daily maximum temperature T_{max} and daily maximum wet–bulb temperature TW_{max} are displayed in Figures 6 and 7. The return levels follow the north-south gradient of the climatic mean temperatures. The northern parts of the Sindh are hotter than the southern parts. Therefore, different stations have different potential for maximum temperature return levels. The stations located in the North are Jacobabad, Mohenjo-daro, Rohri, Padidan, and Nawabshah. While Hyderabad, Chhor, Karachi, and Badin are sited in the South.

The 2, 5, 10, 20, 50, 100-year RLs estimated in Sindh for station observed T_{max} at time reach over 50°C in Jacobabad, Mohenjo-daro, Padidan, Nawabshah, and over 45°C in Rohri, Hyderabad, Chhor, Karachi, Badin. The ERA Interim T_{max} return levels are at least 3°C to 5°C lower in all stations. However, the ERA Interim T_{max} captures the geographical variability of the field, but cannot estimate the correct magnitude of the events. For example, in Badin the return level of the station T_{max} is 42°C in a 3-year return period, while the ERA Interim show the same value of the return level in a 30-year return period (Figure 6).

The RLs of TW_{max} are over the 35°C in all meteorological stations. As for the ERA Interim RLs of TW_{max} are greater than 30°C for all the stations except Karachi, which has RLs less than 30°C. Here, we see again that the RLs of the ERA Interim TW_{max} are smaller than the RLs of station TW_{max}. For example, in Badin station, the RLs of the station TW_{max} is 38°C in a 4-years return period whereas, the ERA Interim reaches the same RLs in a 15-year return period (Figure 7).

It is important to underline that the bias between the station and the ERA Interim data is rather relevant when one wishes to address the impact of hot climatic extremes to the active crop production in the region. The crops are very sensitive to temperature variations, and even a rise of one degree Celsius can cause detrimental changes in the phenological stages of the crops (Hatfield and Preuger, 2015). Every crop has a certain limit to tolerate the temperature. When temperature exceeds this limit, the crop yield is drastically reduced. In summer, the temperature and humidity increase to an extent that there are high chances of a rapid pests spread in the crops. Sindh produces cotton, wheat, rice, mango, banana, and dates, so a correct estimate of temperature extremes is very important in order to avoid the crops failure and the reproduction of pests. Therefore, we apply the standard bias correction on the ERA Interim data to check the alterations in the return levels and return periods of T_{max} and TW_{max}.

The bias corrected ERA Interim T_{max} and TW_{max}, show improvements in the return levels (RLs), along with a good correspondence in each station. In a maximum temperature T_{max} analysis the RLs of the bias corrected ERA Interim overlap the RLs of the station observations in a range 5-100 years, but do not overlap within a range 2-5years, in the Nawabshah, Hyderabad, Karachi, and Badin. However, the rest of the stations show no overlaps of the return levels in both the bias corrected ERA Interim and station observations. In a wet-bulb temperature TW_{max} analysis, the RLs of the bias corrected ERA Interim overlap the RLs of the station observations in Mohenjo-daro, Hyderabad, Chhor, and Badin at some intervals. While, no overlapping of the RLs is detected in rest of the stations, while they differ at some intervals (Figures 6 and 7).

The 2, 5, 10, 20, 50, 100-year RLs of T_{max} for the bias corrected ERA Interim data are greater than 50°C in Jacobabad, Mohenjo-daro, Padidan, Nawabshah, and greater than 45°C in Rohri, Hyderabad, Chhor, Karachi, Badin. As for the TW_{max}, the 2, 5, 10, 20, 50, 100-year RLs of the bias corrected ERA Interim exceed 35°C in all stations. Figures 6 and 7 show that the ERA Interim time series improves a lot after the bias correction, but the two data sets still have some quantitative differences.

The extremes of daily maximum wet-bulb temperature TW_{max} are estimated as above the human survivability threshold 35°C throughout the region, so the risk of hyperthermia is very high here. The human habitability in such a warm region is already at risk. The most vulnerable people are those who are involve in the everyday outdoor activities like farming, fishing, building construction, athletes, elderly and infants can have heat strokes, dehydration etc. Therefore, an early warning system is necessary in Sindh, to avoid the crop failure, water shortages and casualties due to the heat stress each year.

We also plot the station and bias corrected ERA Interim T_{max}, and TW_{max} return levels spatially for the 5, 10, 25 and 50-year return periods (Figures 8 and 9), as a detailed spatial overview of the temperature extremes in Sindh might be of interest to the policy makers.

4. Summary and Conclusion

The main objective of this study is the assessment of the return levels of the extreme daily maximum temperatures T_{max} and wet-bulb temperatures TW_{max} in Southern Pakistan (Sindh). In addition, the performance of the ERA Interim TW_{max} is compared to the weather station TW_{max} to assess the ability to estimating temperature extremes in Sindh. Moreover, a standard bias correction is applied to the ERA Interim data to improve its performance in representing temperature extremes.

In summary, the Peak Over Threshold (POT) method is applied to the daily T_{max} and TW_{max} data of nine observatories and to the corresponding nearest ERA Interim temperature data. Standard declustering technique is applied to all time series to achieve the independence assumption of extremes. The 90% quantile is the appropriate threshold choice for the weather stations, the ERA Interim and the bias corrected ERA Interim maximum temperature and wet-bulb temperature. A Generalized Pareto Distribution (GPD) is fit to both T_{max} and TW_{max} for all three datasets. The results show that the shape parameter ξ is negative for all stations. The scale parameter σ estimated on weather station temperatures is much closer to the bias corrected ERA Interim estimates than the original ERA Interim data ones. The theoretical absolute maxima of the time series are higher than the observed absolute maxima in all stations. The Q-Q plots are used to assess the GPD fit, which results to be acceptable for both T_{max} and TW_{max} station data as compared to the ERA Interim data. However, the bias corrected ERA Interim shows improved GPD fits than ERA Interim.

Return levels (RLs) of T_{max} and TW_{max} are estimated for the 2, 5, 10, 25, 50, 100-year return periods in all datasets. The RLs of T_{max} estimated using the meteorological station temperatures are greater than 50°C in Jacobabad, Mohenjo-daro, Padidan, Nawabshah, and greater than 45°C in Rohri, Hyderabad, Chhor, Karachi and Badin. While the RLs of TW_{max} in station data are larger than 35°C in the entire Sindh, when using ERA Interim temperatures, they are estimated as greater than 45°C in Northern Sindh and greater than 40°C in southern Sindh. The differences in the RLs using the two datasets are between 3°C and 5°C for both shorter and longer return periods due to the minor variations in the shape and scale parameters. Although the ERA-Interim dataset does not capture well the magnitude of the extremes, but it provides a good representation of their spatial fields.

A simple standard bias correction is applied to the ERA Interim to assess whether the return levels of extremes are better predicted after the rescaling is applied. The bias corrected ERA Interim T_{max} and TW_{max} gives return levels closer to the meteorological stations observed ones than the original ERA Interim return levels at all stations. Although the bias corrected ERA Interim shows a good correspondence with the meteorological station data, some differences remain.

This paper contains novel and beneficial information regarding the assessment of the temperature extremes (T_{max} and TW_{max}) in Sindh, which would help the local administrations to prioritize the regions in terms of adaptations. This research fills the gaps in the literature providing information on T_{max} and TW_{max} extremes in Sindh, which would benefit both public and private stakeholders.

Acknowledgements

We like to thank Climate KIC, for funding this research. This publication is a part of a Climate KIC project "Extreme Events in Pakistan: Physical processes and impacts of changing climate", which belongs to the adaptation services platform of the Climate KIC. Thanks to Pakistan Meteorological Department (PMD) and the European Center for Medium range Weather Forecast (ECMWF) for providing datasets. The R development core team (2015) is acknowledged for providing statistics packages. We would like to thank the DFG Cluster of Excellence CliSAP for partially supporting this research activity.

References

Acero, F. J., García, J. A., Gallego, M. C., Parey, S. and Dacunha-Castelle, D.: Trends in summer extreme temperatures over the Iberian Peninsula using nonurban station data, J. Geophys. Res. Atmos., doi:10.1002/2013JD020590, 2014.

Bramati, M.C., Tarragoni, C., Davoli, L., Raffi, R., Extreme Rainfall in Coastal Metropolitan Areas of Central Italy: Rome and Pescara case studies. *Geografia Fisica e Dinamica Quaternaria*, **37**, pp. 3-13, 2014.

Brunetti, M., Maugeri, M., Monti, F. and Nanni, T.: Temperature and precipitation variability in Italy in the last two centuries from homogeneized instrumental time series, J. Climatol., 26(3), 345–381, doi:10.1002/joc.1251, 2006.

Burgueño, A., Lana, X. and Serra, C.: Significant hot and cold events at the Fabra Observatory, Barcelona (NE Spain), Theor. Appl. Climatol., doi:10.1007/s007040200001, 2002.

Brunetti, M., Maugeri, M., Monti, F. and Nanni, T.: Temperature and precipitation variability in Italy in the last two centuries from homogeneized instrumental time series, J. Climatol., 26(3), 345–381, doi:10.1002/joc.1251, 2006.

Brown, S. J., Caesar, J. and Ferro, C. A. T.: Global changes in extreme daily temperature since 1950, J. Geophys. Res. Atmos., doi:10.1029/2006JD008091, 2008.

Chaudhry, Q.-U.-Z. and Rasul, G.: AGRO-CLIMATIC CLASSIFICATION OF PAKISTAN, Q. Sci. Vis., 9(12), 3–4, 2004.

Chaudhry, Q. Z., Rasul, G., Kamal, A., Ahmad Mangrio, M. and Mahmood, S.: Government of Pakistan Ministry of Climate Change Technical Report on Karachi Heat wave June 2015.

Choi, G., Collins, D., Ren, G., Trewin, B., Baldi, M., Fukuda, Y., Afzaal, M., Pianmana, T., Gomboluudev, P., Huong, P. T. T., Lias, N., Kwon, W.-T., Boo, K.-O., Cha, Y.-M. and Zhou, Y.: Changes in means and extreme events of temperature and precipitation in the Asia-Pacific Network region, 1955-2007, Int. J. Climatol., 29(13), 1906–1925, doi:10.1002/joc.1979, 2009.

Christidis, N., Stott, P. A., Brown, S., Hegerl, G. C. and Caesar, J.: Detection of changes in temperature extremes during the second half of the 20th century, Geophys. Res. Lett., doi:10.1029/2005GL023885, 2005.

Christidis, N., Stott, P. A., Zwiers, F. W., Shiogama, H. and Nozawa, T.: Probabilistic estimates of recent changes in temperature: A multi-scale attribution analysis, Clim. Dyn., doi:10.1007/s00382-009-0615-7, 2010.

Coles, S.: An Introduction to Statistical Modeling of Extreme Values, Springer London, London., 2001.

Coelho, C. A. S., Ferro, C. A. T., Stephenson, D. B. and Steinskog, D. J.: Methods for Exploring Spatial and Temporal Variability of Extreme Events in Climate Data, J. Clim., 21(10), 2072–2092, doi:10.1175/2007JCLI1781.1, 2008.

Davison, A. C. and Smith, R. L.: Models for Exceedances over High Thresholds, J. R. Stat. Soc. Ser. B, 52(3), 393–442, doi:10.2307/2345667, 1990.

Dee, D. P., Uppala, S. M., Simmons, A. J., Berrisford, P., Poli, P., Kobayashi, S., Andrae, U., Balmaseda, M. A., Balsamo, G., Bauer, P., Bechtold, P., Beljaars, A. C. M., van de Berg, L., Bidlot, J., Bormann, N., Delsol, C., Dragani, R., Fuentes, M., Geer, A. J., Haimberger, L., Healy, S. B., Hersbach, H., Hólm, E. V., Isaksen, L., Kållberg, P., Köhler, M., Matricardi, M., Mcnally, A. P., Monge-Sanz, B. M., Morcrette, J. J., Park, B. K., Peubey, C., de Rosnay, P., Tavolato, C., Thépaut, J. N. and Vitart, F.: The ERA-Interim reanalysis: Configuration and performance of the data assimilation system, Q. J. R. Meteorol. Soc., doi:10.1002/qj.828, 2011.

Deidda, R. and Puliga, M.: Sensitivity of goodness-of-fit statistics to rainfall data rounding off, Phys. Chem. Earth, doi:10.1016/j.pce.2006.04.041, 2006.

Dickey, D. A. and Fuller, W. A.: Distribution of the Estimators for Autoregressive Time Series With a Unit Root, J. Am. Stat. Assoc., 74(366), 427, doi:10.2307/2286348, 1979.

Faranda, D., Lucarini, V., Turchetti, G. and Vaienti, S.: Numerical Convergence of the Block-Maxima Approach to the Generalized Extreme Value Distribution, J. Stat. Phys., doi:10.1007/s10955-011-0234-7, 2011.

Ferro, C. A. T. and Segers, J.: Inference for clusters of extreme values, J. R. Stat. Soc. B, 65(2), 545–556, 2003.

Frich, P., Alexander, L. V., Della-Marta, P., Gleason, B., Haylock, M., Tank Klein, A. M. G. and Peterson, T.: Observed coherent changes in climatic extremes during the second half of the twentieth century, Clim. Res., doi:10.3354/cr019193, 2002.

Furrer, E., Katz, R., Walter, M. and Furrer, R.: Statistical modeling of hot spells and heat waves, Clim. Res., 43(3), 191–205, doi:10.3354/cr00924, 2010.

Ghil, M., Yiou, P., Hallegatte, S., Malamud, B. D., Naveau, P., Soloviev, A., Friederichs, P., Keilis-Borok, V., Kondrashov, D., Kossobokov, V., Mestre, O., Nicolis, C., Rust, H. W., Shebalin, P., Vrac, M., Witt, A. and Zaliapin, I.: Extreme events: Dynamics, statistics and prediction, Nonlinear Process. Geophys., doi:10.5194/npg-18-295-2011, 2011.

Hatfield, J. L. and Prueger, J. H.: Temperature extremes: Effect on plant growth and development, Weather Clim. Extrem., doi:10.1016/j.wace.2015.08.001, 2015.

Imtiaz S, Rehman, ZU. 2015. June 25. Death Toll From Heat Wave in Karachi, Pakistan, Hits 1,000. *The New York Times* retrieved from http://www.nytimes.com/2015/06/26/world/asia/karachi-pakistan-heat-wave-deaths.html?_r=0

IPCC: Managing the Risks of Extreme Events and Disasters to Advance Climate Change Adaptation, edited by C. B. Field, V. Barros, T. F. Stocker, and Q. Dahe, Cambridge University Press, Cambridge., 2012.

Islam, S. U., Rehman, N. and Sheikh, M. M.: Future change in the frequency of warm and cold spells over Pakistan simulated by the PRECIS regional climate model, Clim. Change, doi:10.1007/s10584-009-9557-7, 2009.

Klein Tank, A. M. G., Peterson, T. C., Quadir, D. A., Dorji, S., Zou, X., Tang, H., Santhosh, K., Joshi, U. R., Jaswal, A. K. and Kolli, R. K.: Changes in daily temperature and precipitation extremes in central and south Asia, J. Geophys. Res, 111, doi:10.1029/2005JD006316, 2006.

Klein Tank, A.M.G., Zwiers, F.W., Zhang, X.,: Guidelines on Analysis of extremes in a changing climate in support of informed decisions for adaptation., 2009.

Leadbetter, M. R.: Extremes and local dependence in stationary sequences, Zeitschrift f??r Wahrscheinlichkeitstheorie und Verwandte Gebiete, doi:10.1007/BF00532484, 1983.

Loynes, R. M.: Extreme Values in Uniformly Mixing Stationary Stochastic Processes, Ann. Math. Stat., 36(3), 993–999, doi:10.1214/aoms/1177700071, 1965.

Lucarini, V., Faranda, D., Wouters, J. and Kuna, T.: Towards a General Theory of Extremes for Observables of Chaotic Dynamical Systems., J. Stat. Phys., 154, 723–750, doi:10.1007/s10955-013-0914-6, 2014.

Lucarini, V., Faranda, D., .Freitas, A.C.M., Freitas, J.M., Holland, M., Kuna, T., Nicol, M., Todd, M., Vaienti, S.: Extremes and Recurrence in Dynamical Systems, *John Wiley & Sons Inc, Engelska,*2016.

Lustenberger, A., Knutti, R. and Fischer, E. M.: The potential of pattern scaling for projecting temperature-related extreme indices, Int. J. Climatol., 34(1), 18–26, doi:10.1002/joc.3659, 2014.

Morak, S., Hegerl, G. C. and Kenyon, J.: Detectable regional changes in the number of warm nights, Geophys. Res. Lett., doi:10.1029/2011GL048531, 2011.

Morak, S., Hegerl, G. C. and Christidis, N.: Detectable changes in the frequency of temperature extremes, J. Clim., doi:10.1175/JCLI-D-11-00678.1, 2013.

Newell, G. F.: Asymptotic Extremes for m-Dependent Random Variables, Ann. Math. Stat., 35(3), 1322–1325, doi:10.1214/aoms/1177703288, 1964.

Nogaj, M., Yiou, P., Parey, S., Malek, F. and Naveau, P.: Amplitude and frequency of temperature extremes over the North Atlantic region, Geophys. Res. Lett., doi:10.1029/2005GL024251, 2006.

Pachauri, R. K., Meyer, L., Van Ypersele, J.-P., Brinkman, S., Van Kesteren, L., Leprince-Ringuet, N. and Van Boxmeer, F.: Climate Change 2014 Synthesis Report The Core Writing Team Core Writing Team Technical Support Unit for the Synthesis Report, IPCC., n.d, 2014.

Pakistan Meteorological Department, Monthly Climatic Normal of Pakistan (1980-2010), Climate Data Processing Centre (CDPC), Karachi, 2013.

Pal, J. S. and Eltahir, E. A. B.: Future temperature in southwest Asia projected to exceed a threshold for human adaptability, , doi:10.1038/NCLIMATE2833, 2015.

Rasul, G., Mahmood, A., Sadiq, A. and Khan, S. I.: Vulnerability of the Indus Delta to Climate Change in Pakistan, Pakistan J. Meteorol., 8(16), 2012.

Rasul, G., Afzal, M., Zahid, M., Ahsan, S. and Bukhari, A.: Climate Change in Pakistan Focused on Sindh Province., 2012.

R Development Core Team,. R, a language and environment for statistical computing. R Foundation for Statistical Computing, Vienn, Austria, 2015.

Sheridan, S.C., Allen M. J., Changes in the Frequency and Intensity of Extreme Temperature Events and Human Health Concerns. *Current Climate Change Reports* **1**(3): 155-162, doi:10.1007/s40641-015-0017-3, 2015.

Sherwood, S. C. and Huber, M.: An adaptability limit to climate change due to heat stress, Proc. Natl Acad. Sci. USA 107 9552–5, 2010.

Scarrott, C. and Macdonald, A.: A REVIEW OF EXTREME VALUE THRESHOLD ES- TIMATION AND UNCERTAINTY QUANTIFICATION, REVSTAT – Stat. J., 10(1), 33–60, 2012.

Smith, R. L.: Extreme Value Analysis of Environmental Time Series: An Application to Trend Detection in Ground-Level Ozone, Stat. Sci., 4(4), 367–377, doi:10.1214/ss/1177012400, 1989.

Stull, R.: Wet-bulb temperature from relative humidity and air temperature, J. Appl. Meteorol. Climatol.,

Earth Syst. Dynam. Discuss., doi:10.5194/esd-2016-72, 2017
Manuscript under review for journal Earth Syst. Dynam.
Published: 2 January 2017

doi:10.1175/JAMC-D-11-0143.1, 2011.

Tebaldi, C., Hayhoe, K., Arblaster, J. M. and Meehl, G. A.: Going to the extremes: An intercomparison of model-simulated historical and future changes in extreme events, Clim. Change, doi:10.1007/s10584-006-9051-4, 2006.

Zahid, M. and Rasul, G.: Rise in Summer Heat Index over Pakistan, Pakistan J. Meteorol., 6(12), 2010.

Zahid, M. and Rasul, G.: Changing trends of thermal extremes in Pakistan, Clim. Change, doi:10.1007/s10584-011-0390-4, 2012.

Zhang, X.B., Zwiers, F.W., Li, G.L., Monte Carlo experiments on the detection of trends in extreme values, *J. Clim.* **17**:1945– 1952, 2004.

Zwiers, F. W., Zhang, X. and Feng, Y.: Anthropogenic influence on long return period daily temperature extremes at regional scales, J. Clim., doi:10.1175/2010JCLI3908.1, 2011.

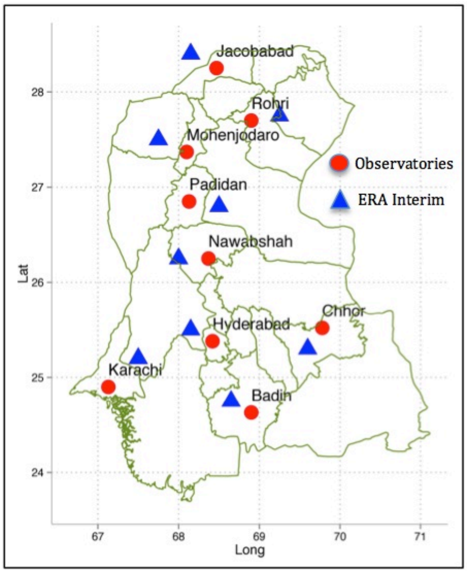

Figure 1: Study Domain (23.5 – 28.5° N , 66.5- 71.1°E)

Table 1. Code, Name, Geographic coordinates and Altitude of the stations.

Code	Name	PMD weather stations			ERA-Interim stations	
		Latitude	Longitude	Altitude (m)	Latitude	Longitude
JCB	Jacobabad	28° 18'N	68° 28'E	55	28 °4'N	68 °15'E
MJD	Mohenjo-daro	27° 22'N	68° 06'E	52.1	27°5'N	67 °75'E
RHI	Rohri	27° 40'N	68° 54'E	66	27°75'N	69 °25'E
PDN	Padidan	26° 51'N	68° 08'E	46	26°8'N	68 °5'E
NWB	Nawabshah	26° 15'N	68° 22'E	37	26°25'N	68 °0'E
HYD	Hyderabad	25° 23'N	68° 25'E	40	25°5'N	68 °15'E
CHR	Chhor	29° 31'N	69° 47' E	5	25°3'N	69 °6'E
KHI	Karachi	24° 54'N	67°08' E	21	25°2'N	67 °5'E
BDN	Badin	24° 38'N	68° 54'E	10	24 °75'N	68 °65'E

Table 2. Monthly mean climatic characteristics of all nine stations from1980-2010.

Stations	Mean Temperature (°C)												
	Jan	Feb	Mar	Apr	May	Jun	Jul	Aug	Sep	Oct	Nov	Dec	Annual
Jacobabad	15.2	18.2	24	30.5	35.6	37	34.8	33	31.4	27.8	22.3	16.7	27
Mohenjo-daro	13.9	16.7	23	29.1	34.1	35	33.9	32.9	30.9	26.7	21.1	15.9	25.9
Rohri	15.6	18.2	23.6	29.8	34.5	35.6	33.9	32.3	31.2	27.6	22.1	16.9	26.4
Padidan	14.8	17.7	23.5	29.9	34.4	35.5	33.7	32.1	31	27.5	22.4	16.4	26.5
Nawabshah	15.4	18	24	29.8	34.5	35.6	34	32.3	31.5	28	22.4	16.9	26.7
Hyderabad	18	21	26.2	30.9	33.3	34	32.4	31.1	31	29.6	24.8	19.6	27.6
Chhor	16.5	19.5	25	30.1	33.5	33.7	31.6	30.1	30.1	28.2	22.6	17.9	26.3
Karachi	18.6	21.2	25.4	28.9	31.1	31.9	30.5	29.2	29.5	28.9	24.6	20.4	26.4
Badin	17.5	20.5	25.8	30.1	32.6	32.8	31	29.6	29.6	28.7	24	19	26.6
Stations	**Minimum Temperature (°C)**												
	Jan	**Feb**	**Mar**	**Apr**	**May**	**Jun**	**Jul**	**Aug**	**Sep**	**Oct**	**Nov**	**Dec**	**Annual**
Jacobabad	7.9	10.9	16.6	22.4	27.4	29.8	29.3	28.4	26.3	20.5	14.3	8.9	19.9
Mohenjo-daro	4.7	7.9	13.3	18.9	24	27.4	27.9	27	24.7	18.2	11.8	7.3	17.3
Rohri	8.3	10.8	15.9	21.7	26.1	27.7	27.1	26	24.4	19.9	14.2	9.6	18.7
Padidan	6.5	8.9	14.5	20.2	24.7	27	26.9	25.8	23.7	18.3	12.4	7.6	17.8
Nawabshah	6.3	8.7	14.2	19.4	24.6	27.3	27.2	25.9	23.8	18.4	12.4	7.8	17.9
Hyderabad	11.4	13.9	18.8	22.8	26.1	27.9	27.6	26.5	25.4	22.5	17.4	13	21.1
Chhor	5.9	8.9	14.8	20.3	24.8	26.9	26.5	25.3	23.9	18.7	11.8	7	17.6
Karachi	11.5	14	18.6	23	26.6	28.3	27.6	26.3	25.6	21.9	16.8	12.7	20.7
Badin	9.9	12.6	17.9	22.3	25.7	27.6	27.1	26	25	22.1	16.5	11.4	20.2
Stations	**Maximum Temperature (°C)**												
	Jan	**Feb**	**Mar**	**Apr**	**May**	**Jun**	**Jul**	**Aug**	**Sep**	**Oct**	**Nov**	**Dec**	**Annual**
Jacobabad	22.6	25.6	31.4	38.6	43.9	44.4	40.2	37.6	36.8	35.1	30.3	24.4	34.1
Mohenjo-daro	23.1	26.2	32.1	38.7	43.8	44.2	40.9	38.7	37.5	35.2	30.5	24.8	34.5
Rohri	22.6	25.6	31.2	38.1	43	43.5	40.5	38.3	37.8	35.2	30	24.3	34
Padidan	23.1	26.4	32.2	39.4	43.9	44.1	40.6	38.4	38.3	36.3	31.1	25.3	34.8
Nawabshah	24.5	27.9	33.8	40.2	44.2	43.9	40.7	38.8	39	37.7	32.3	26.1	35.5
Hyderabad	24.7	28.1	33.7	38.8	41.3	40	37.2	35.6	36.3	36.7	31.9	26.2	34.1
Chhor	26.9	29.9	35.2	40	42	40.6	36.8	34.9	36.3	37.6	33.5	28.7	35
Karachi	26.3	28.4	32.2	34.7	35.5	35.4	33.3	32.1	33.2	35.5	32.5	28.2	32
Badin	25.2	28.3	33.7	37.8	39.4	37.9	34.9	33.2	34.2	35.2	31.4	26.5	32.9

Earth Syst. Dynam. Discuss., doi:10.5194/esd-2016-72, 2017
Manuscript under review for journal Earth Syst. Dynam.
Published: 2 January 2017

Earth System Dynamics
Discussions
Open Access

Table 3. Results of the Kolmogorov-Smirnov Goodness of fit test and Anderson-Darling test between empirical and GPD fits.

Observed T*max*

Test Statistics	Null Hypothesis	*P*-value								
		JAC	**MJD**	**RHI**	**PDN**	**NWS**	**HYD**	**CHR**	**KHI**	**BDN**
Kolmogorov Smirnov	Equality of probability distribution	0.947	0.340	0.996	0.139	0.941	0.385	0.928	0.306	0.666
Anderson Darling	Equality of probability distribution	0.553	0.978	0.654	0.857	0.157	0.649	0.233	0.869	0.145

ERA Interim T*max*

Test Statistics	Null Hypothesis	*P*-value								
		JAC	**MJD**	**RHI**	**PDN**	**NWS**	**HYD**	**CHR**	**KHI**	**BDN**
Kolmogorov Smirnov	Equality of probability distribution	0.169	0.125	0.553	0.456	0.322	0.187	0.419	0.456	0.332
Anderson Darling	Equality of probability distribution	0.355	0.263	0.165	0.587	0.615	0.398	0.266	0.687	0.425

Bias corrected ERA Interim T*max*

Test Statistics	Null Hypothesis	*P*-value								
		JAC	**MJD**	**RHI**	**PDN**	**NWS**	**HYD**	**CHR**	**KHI**	**BDN**
Kolmogorov Smirnov	Equality of probability distribution	0.452	0.4729	0.197	0.489	0.269	0.137	0.158	0.243	0.312
Anderson Darling	Equality of probability distribution	0.352	0.315	0.235	0.270	0.335	0.289	0.216	0.390	0227

Observed TW*max*

Test Statistics	Null Hypothesis	*P*-value								
		JAC	**MJD**	**RHI**	**PDN**	**NWS**	**HYD**	**CHR**	**KHI**	**BDN**
Kolmogorov Smirnov	Equality of probability distribution	0.981	0.111	0.341	0.226	0.457	0.545	0.441	0.385	0.211
Anderson Darling	Equality of probability distribution	0.623	0.745	0.587	0.884	0.199	0.123	0.789	0.669	0.473

ERA Interim TW*max*

Test Statistics	Null Hypothesis	*P*-value								
		JAC	**MJD**	**RHI**	**PDN**	**NWS**	**HYD**	**CHR**	**KHI**	**BDN**
Kolmogorov Smirnov	Equality of probability distribution	0.712	0.564	0.955	0.425	0.258	0.134	0.856	0.497	0.222
Anderson Darling	Equality of probability distribution	0.236	0.474	0.516	0.219	0.356	0.117	0.537	0.464	0.613

Bias corrected ERA Interim TW*max*

Test Statistics	Null Hypothesis	*P*-value								
		JAC	**MJD**	**RHI**	**PDN**	**NWS**	**HYD**	**CHR**	**KHI**	**BDN**
Kolmogorov Smirnov	Equality of probability distribution	0.268	0.688	0.127	0.372	0.268	0.229	0.591	0.582	0.478
Anderson Darling	Equality of probability distribution	0.373	0.484	0.278	0.432	0.306	0.283	0.365	0.445	0.483

Table 4. Estimated parameters shape ξ, scale σ and standard error Δξ of all the data sets.

Station observed T_{max}									
Estimates	**JCB**	**MJD**	**RHI**	**PDN**	**NWB**	**HYD**	**CHR**	**KHI**	**BDN**
Shape ξ	-0.3875	-0.2550	-0.4182	-0.3261	-0.3323	-0.3292	-0.3108	-0.2225	-0.3292
Standard Error Δξ	0.0317	0.0226	0.0226	0.0218	0.0208	0.0312	0.0371	0.0341	0.0312
Scale σ	2.7540	2.0819	2.3510	2.2144	2.1391	2.2286	2.5629	2.5685	2.2286
Standard Error Δσ	0.1421	0.1040	0.1075	0.1076	0.1031	0.1166	0.1462	0.1444	0.1166
ERA Interim T_{max}									
Estimates	**JCB**	**MJD**	**RHI**	**PDN**	**NWB**	**HYD**	**CHR**	**KHI**	**BDN**
Shape ξ	-0.1959	-0.1788	-0.2076	-0.2185	-0.2135	-0.3380	-0.2850	-0.0376	-0.2514
Standard Error Δξ	0.0320	0.0348	0.0343	0.0287	0.0265	0.0316	0.0337	0.0508	0.0371
Scale σ	1.4643	1.3230	1.3440	1.5045	1.5630	2.0656	1.8497	1.3303	2.0410
Standard Error Δσ	0.0798	0.0739	0.0741	0.0788	0.0788	0.1082	0.0949	0.0908	0.1153
Bias Corrected ERA Interim T_{max}									
Estimates	**JCB**	**MJD**	**RHI**	**PDN**	**NWB**	**HYD**	**CHR**	**KHI**	**BDN**
Shape ξ	-0.1959	-0.1788	-0.2076	-0.2185	-0.2135	-0.3380	-0.2850	-0.0376	-0.2514
Standard Error Δξ	0.0320	0.0348	0.0343	0.0287	0.0265	0.0316	0.0337	0.0508	0.0371
Scale σ	1.9834	1.7918	1.8205	2.0382	2.1164	2.7980	2.3081	1.8016	2.7636
Standard Error Δσ	0.1081	0.1001	0.1004	0.1068	0.1068	0.1467	0.1233	0.1229	0.1562
Station observed TW_{max}									
Estimates	**JCB**	**MJD**	**RHI**	**PDN**	**NWB**	**HYD**	**CHR**	**KHI**	**BDN**
Shape ξ	-0.1769	-0.1860	-0.2150	-0.2157	-0.2164	-0.3231	-0.2423	-0.2190	-0.1867
Standard Error Δξ	0.0383	0.0354	0.0347	0.0442	0.0266	0.0269	0.0347	0.0368	0.0322
Scale σ	2.7590	2.0454	1.9600	2.0780	1.8572	2.3724	2.5126	2.3375	1.9032
Standard Error Δσ	0.1596	0.1146	0.1084	0.1289	0.0938	0.1191	0.1380	0.1328	0.1055
ERA Interim TW_{max}									
Estimates	**JCB**	**MJD**	**RHI**	**PDN**	**NWB**	**HYD**	**CHR**	**KHI**	**BDN**
Shape ξ	-0.0896	-0.0946	-0.0687	-0.1257	-0.1583	-0.1771	-0.0902	-0.0194	-0.1733
Standard Error Δξ	0.0379	0.0293	0.0327	0.0342	0.0313	0.0377	0.0357	0.0359	0.0378
Scale σ	1.2879	1.2437	1.2311	1.4408	1.6104	1.6499	1.3423	0.6801	1.7886
Standard Error Δσ	0.0748	0.0660	0.0676	0.0804	0.0875	0.0959	0.0760	0.0398	0.1028
Bias Corrected ERA Interim TW_{max}									
Estimates	**JCB**	**MJD**	**RHI**	**PDN**	**NWB**	**HYD**	**CHR**	**KHI**	**BDN**
Shape ξ	-0.08961	-0.0946	-0.06870	-0.12570	-0.15831	-0.17711	-0.09017	-0.01942	-0.17332
Standard Error Δξ	0.03786	0.02931	0.03275	0.03424	0.03134	0.03767	0.03571	0.03593	0.03782
Scale σ	1.35674	1.64650	1.75852	1.49477	1.52013	2.05281	2.14609	1.39943	2.15299
Standard Error Δσ	0.07878	0.08736	0.09651	0.08347	0.08254	0.11924	0.12145	0.08193	0.12370

Earth Syst. Dynam. Discuss., doi:10.5194/esd-2016-72, 2017
Manuscript under review for journal Earth Syst. Dynam.
Published: 2 January 2017

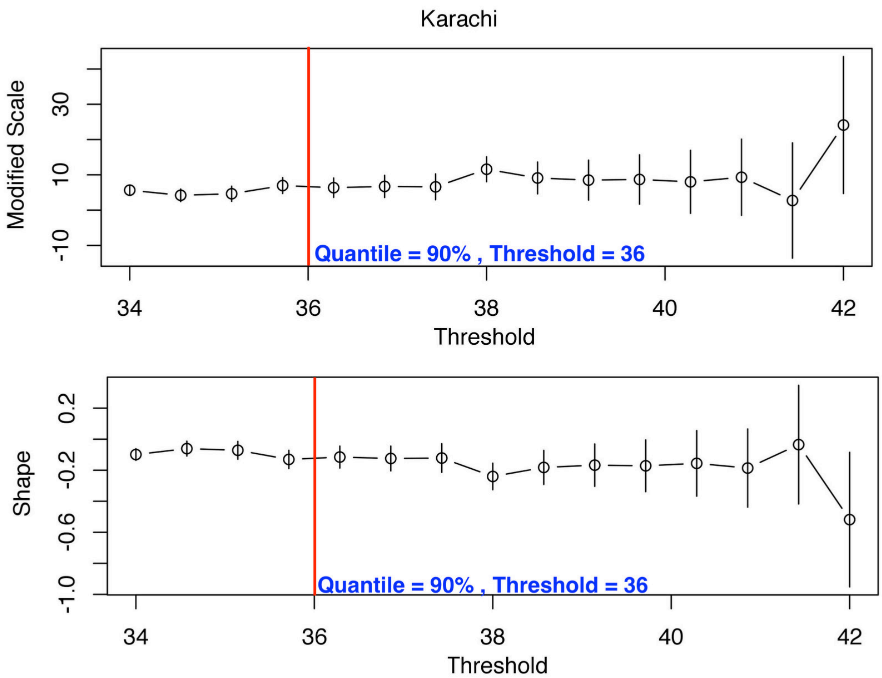

Figure 2. Modified scale (σ^*) and shape parameter (ξ) of the observed T_{max} Karachi. The red vertical lines represent the selected threshold according to the station quantiles.

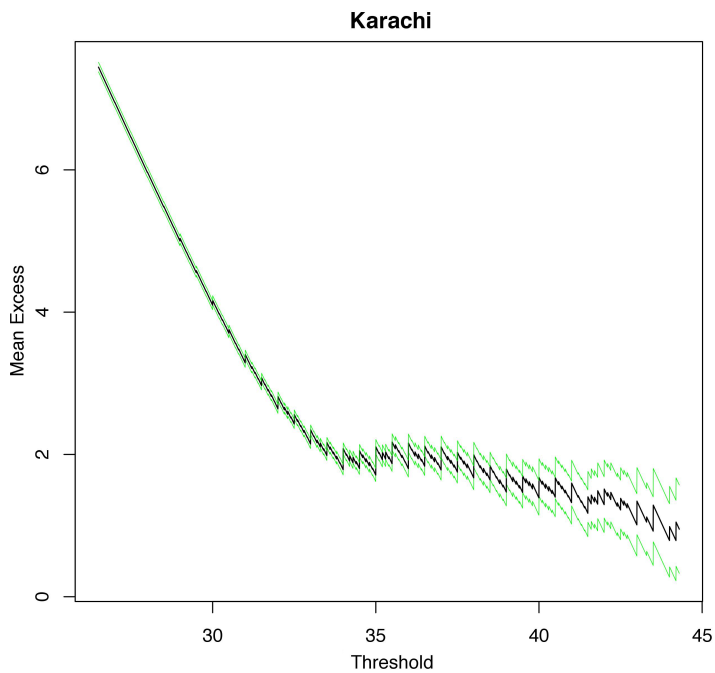

Figure 3. Mean residual life plot of the station observed T_{max} Karachi.

Earth Syst. Dynam. Discuss., doi:10.5194/esd-2016-72, 2017
Manuscript under review for journal Earth Syst. Dynam.
Published: 2 January 2017

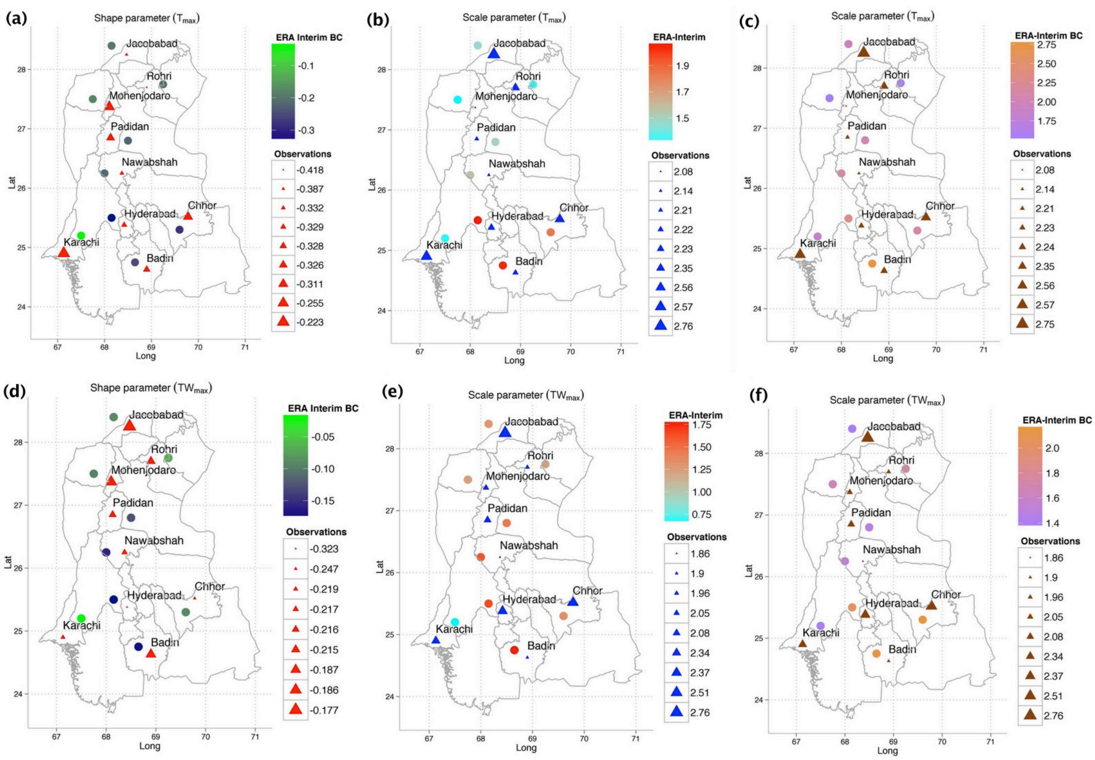

Figure 4. Spatial distribution of the shape parameters ξ and scale parameters σ of the station observed, ERA Interim, and bias corrected ERA Interim T_{max} (upper panel) and TW_{max} (lower panel).

Earth Syst. Dynam. Discuss., doi:10.5194/esd-2016-72, 2017
Manuscript under review for journal Earth Syst. Dynam.
Published: 2 January 2017

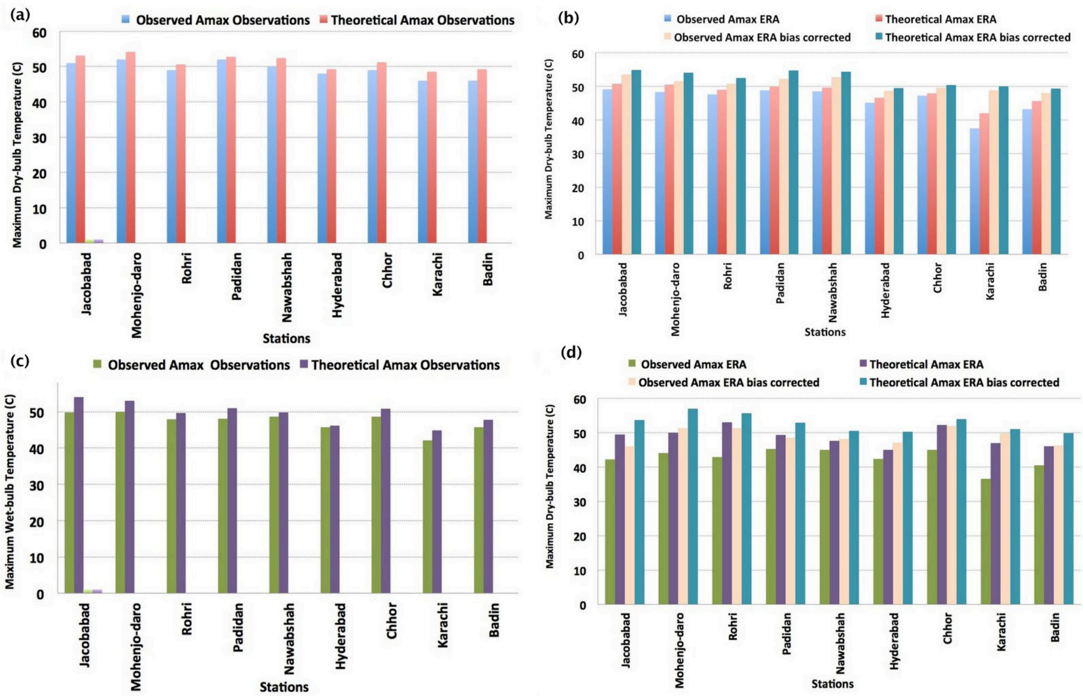

Figure 5. Absolute maxima A_{max} (a) station observed T_{max} (b) ERA Interim and bias corrected ERA Interim T_{max} (c) station observed TW_{max} (d) ERA Interim and bias corrected ERA Interim TW_{max}

Earth Syst. Dynam. Discuss., doi:10.5194/esd-2016-72, 2017
Manuscript under review for journal Earth Syst. Dynam.
Published: 2 January 2017

Earth System Dynamics
Discussions
Open Access

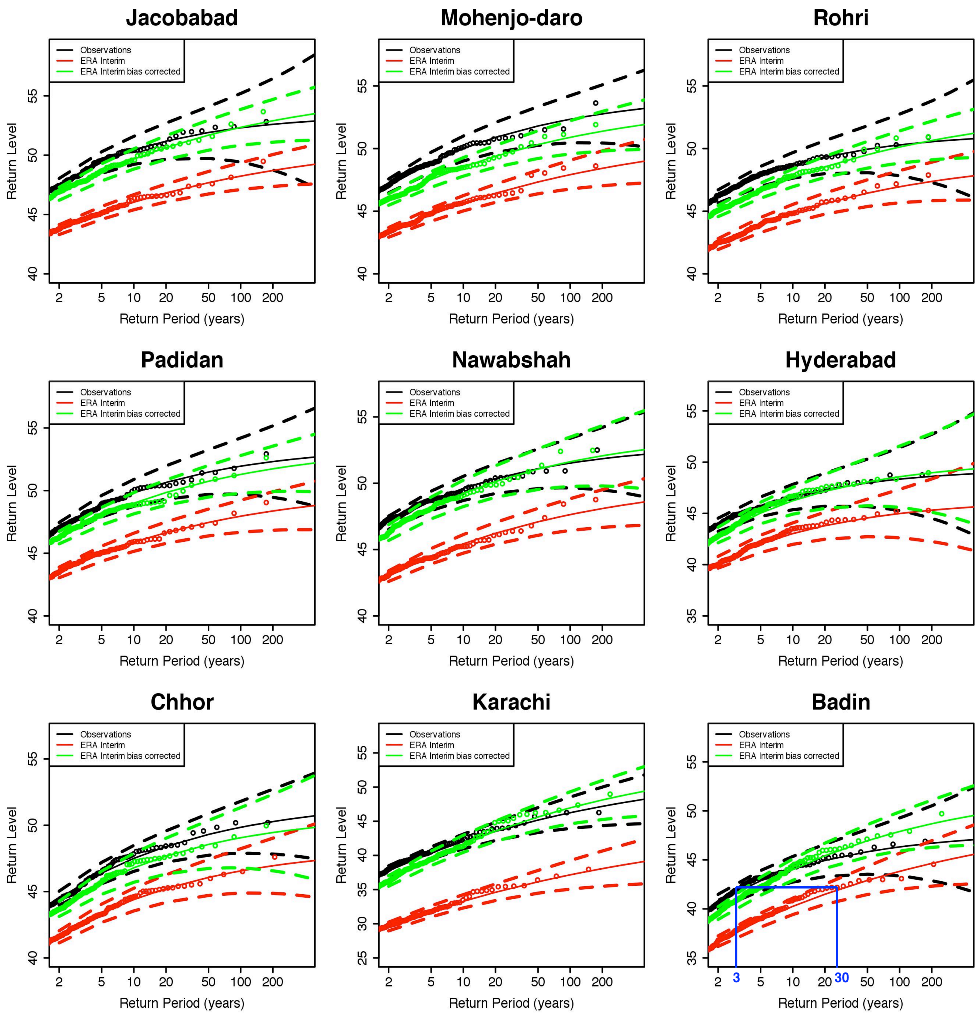

Figure 6. Return level plots of the station observed T_{max} (black) , ERA Interim T_{max} (red), and bias corrected ERA Interim T_{max} (green) in degree Celsius. The blue line is to show a difference in the observed and ERA Interim RLs.

Earth System Dynamics
Discussions
Open Access

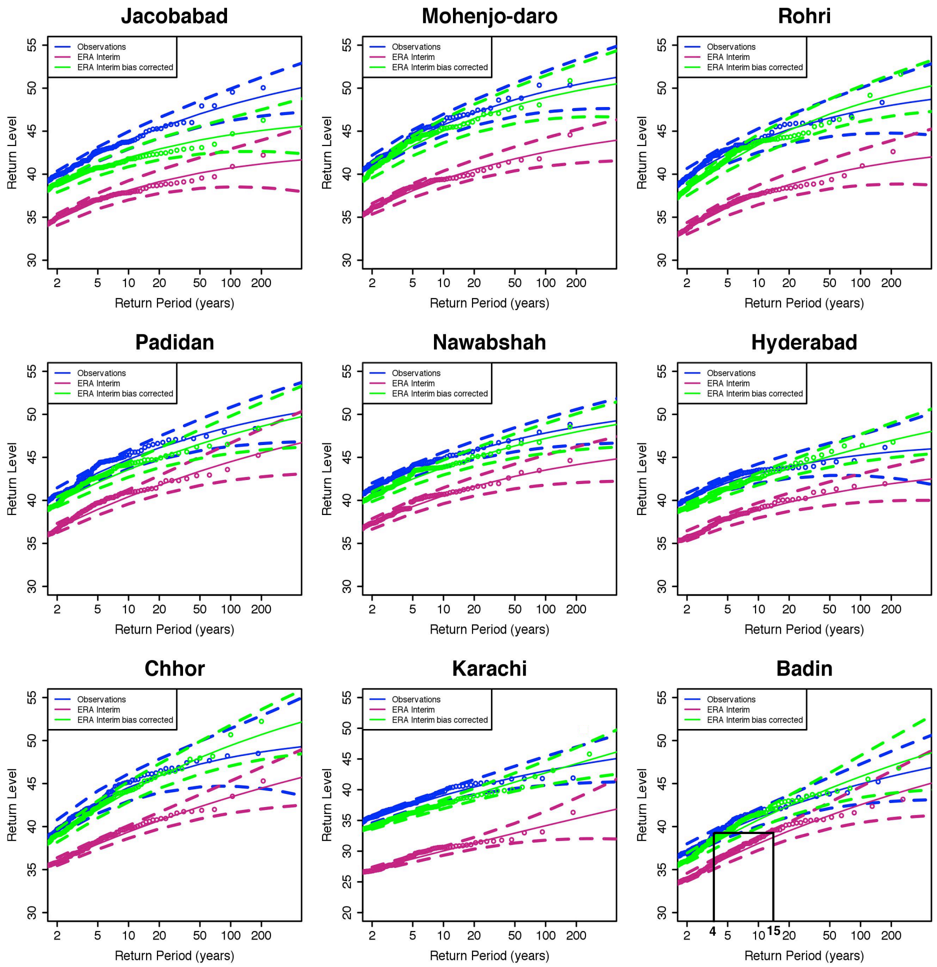

Figure 7. Return level plots of the station observed TW_{max} (blue), ERA Interim T_{max} (pink), and bias corrected ERA Interim T_{max} (green) in degree Celsius. The black line is to show a difference in the observed and ERA Interim RLs.

Earth Syst. Dynam. Discuss., doi:10.5194/esd-2016-72, 2017
Manuscript under review for journal Earth Syst. Dynam.
Published: 2 January 2017

Earth System Dynamics
Discussions
Open Access

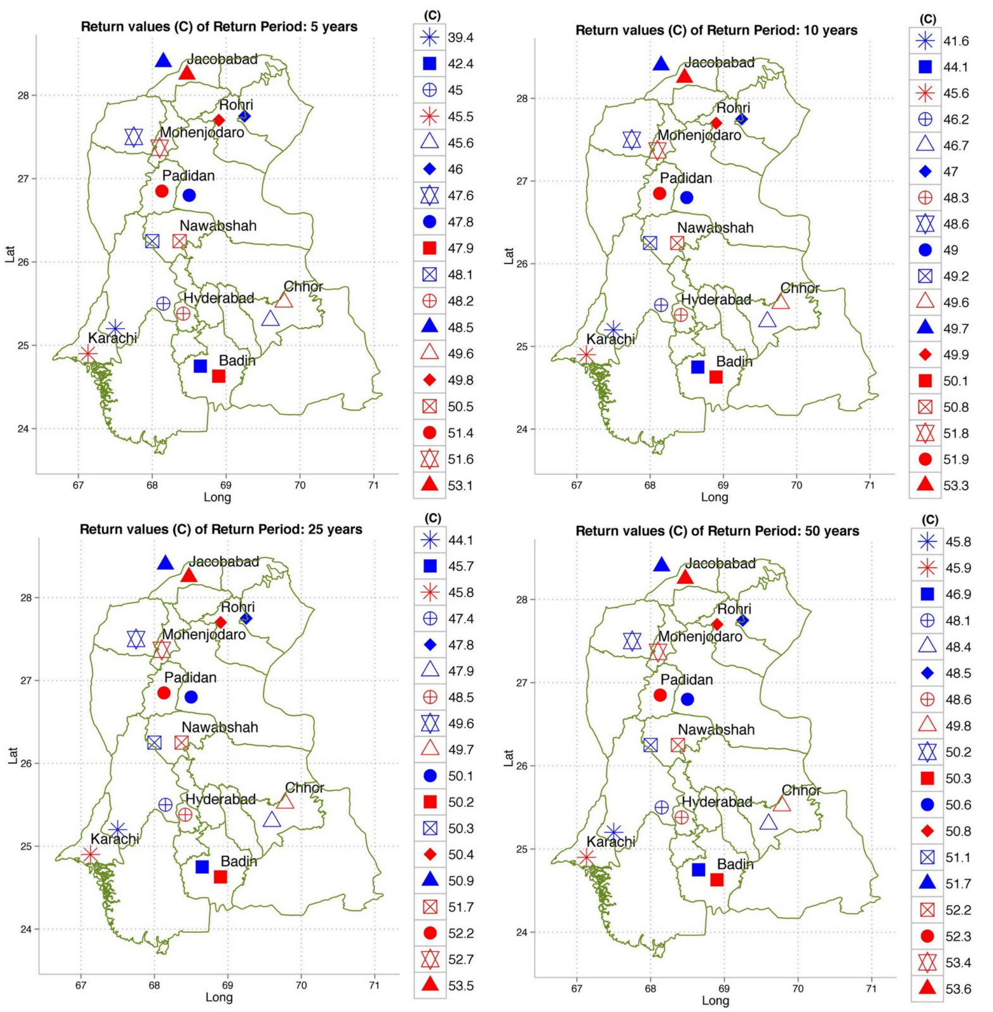

Figure 8. Spatial distribution of the station observed T_{max} (red) and bias corrected ERA Interim T_{max} (blue) return levels corresponding to return periods of 5, 10, 25 and 50 years in southern Pakistan.

Earth Syst. Dynam. Discuss., doi:10.5194/esd-2016-72, 2017
Manuscript under review for journal Earth Syst. Dynam.
Published: 2 January 2017

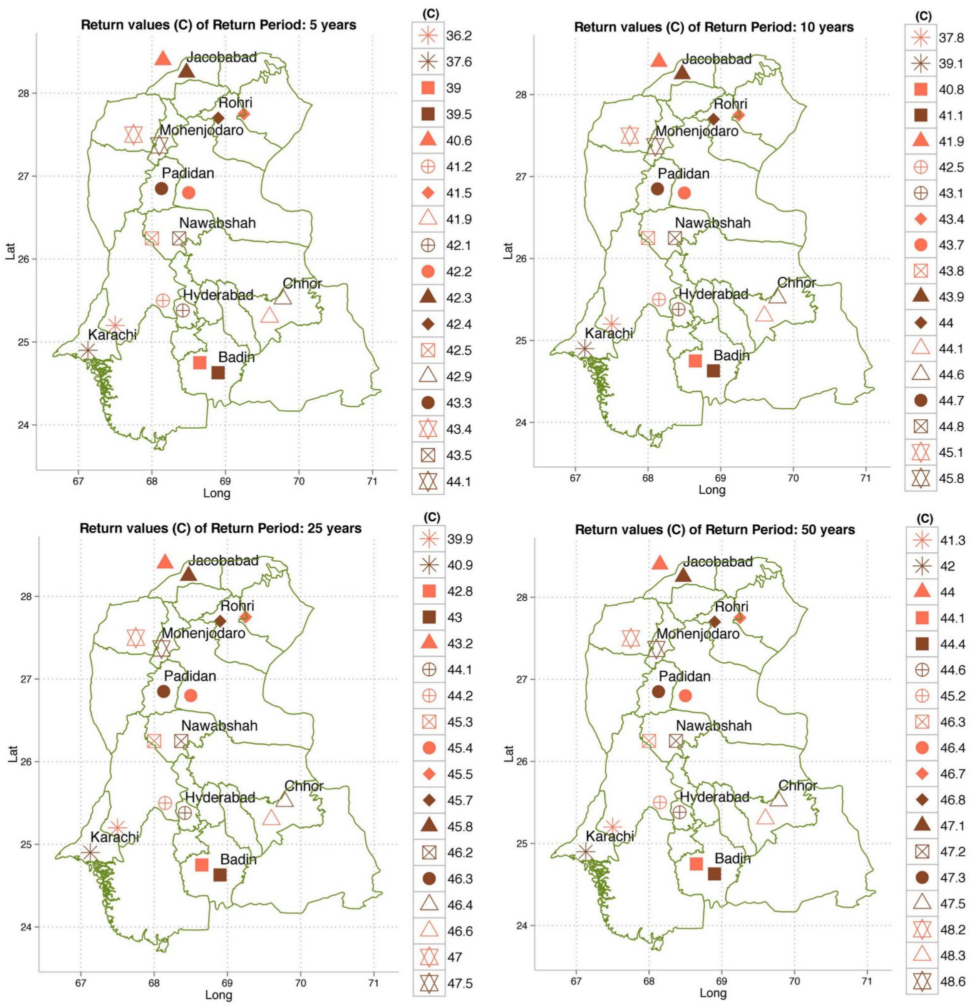

Figure 9. Spatial distribution of the station observed TW_{max} (brown) and bias corrected ERA Interim TW_{max} (orange) return levels corresponding to return periods of 5, 10, 25 and 50 years in southern Pakistan.